

## Electronic Supplementary Information

### Axially twinned Nanodumbbell with a Pt bar and two Rh@Pt balls designed for high catalytic activity: Transferring the twinned crystallographic structure from the Pt bar to the entire dumbbell

*Nguyen Tien Khi<sup>†</sup>, Jisun Yoon<sup>†</sup>, Heonjo Kim<sup>†</sup>, Sangmin Lee<sup>‡</sup>, Byeongyoon Kim<sup>†</sup>, Hionsuck Baik<sup>†</sup>, Seong Jung Kwon<sup>\*‡</sup>, and Kwangyeol Lee<sup>\*‡</sup>*

<sup>†</sup>Department of Chemistry and Research Institute for Natural Sciences, Korea University, Seoul 136-701 (Korea)

<sup>‡</sup>Department of Chemistry, Konkuk University, Seoul 143-701 (Korea)

<sup>†</sup>Korea Basic Science Institute (KBSI), Seoul 136-713 (Korea)

\* Corresponding authors : kylee1@korea.ac.kr (K. Lee), sjkwon@konkuk.ac.kr (S. J. Kwon)

#### Material Characterizations

Transmission electron microscopy (TEM) and high-resolution TEM (HRTEM) were performed on a TECNAI G2 20 S-Twin operated at 200kV and TECNAI G2 F30 operated at 300 kV. X-ray diffraction (XRD) patterns were collected with a Rigaku Ultima III diffractometer system using a graphite-monochromatized Cu-K $\alpha$  radiation at 40kV and 40mA.

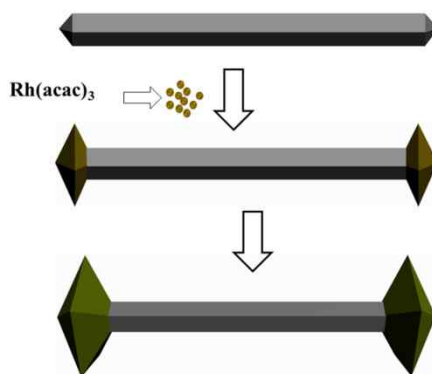
#### Experimental Section

**Preparation of Pt nanorod (Fig. S1a):** The synthetic condition of Pt nanorods was slightly modified from the literature version.<sup>[1]</sup> A slurry of Pt(acac)<sub>2</sub> (0.06 mmol), ethylene glycol (1.86 mmol) and octadecylamine (15 mmol) was prepared in a 15 mL two-neck round bottom flask with a magnetic stirring. After being placed under vacuum for 120 min with magnetic stirring at 80 °C, the resulting solution was recharged by 1 atm CO gas and then was heated up to 150 °C, and kept at that temperature for 120 min under CO gas. Finally, dark brown precipitates could be obtained by cooling down the solution to room temperature and then by centrifugation with added methanol / toluene (v / v = 15 mL / 15 mL).



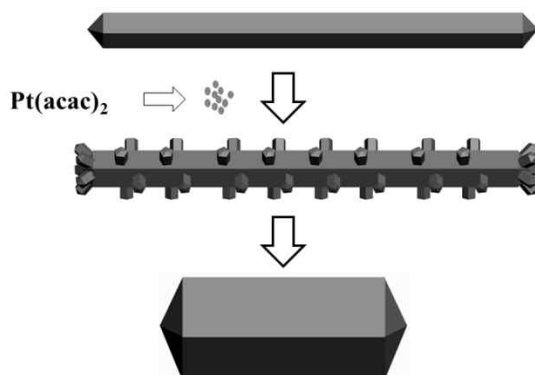
**Preparation of Rh-Pt-Rh barbell and Thermal stability test (Fig. S3):** Pt nanorods (~ 2 mg) were dispersed in a mixture of Rh(acac)<sub>3</sub> (0.05mmol), ethylene glycol (1.86 mmol) and octadecylamine (15 mmol) in a two-neck round bottom flask (15 mL) with a magnetic stirring at 80 °C. After being evacuated for 10 min with stirring at 80 °C, the resulting solution was **heated up to 130 °C for 20 h under Ar gas condition to form Rh-Pt-Rh nanobarbells..**

**[Thermal stability test]** The solution was recharged by CO gas and heated up to 200 °C. Finally, dark brown precipitates could be obtained by cooling down the solution to room temperature and then by centrifugation with added methanol / toluene (v / v = 15 / 15 mL).

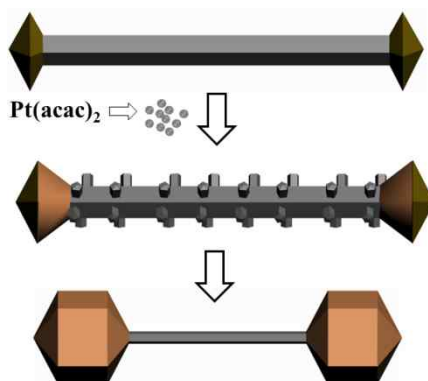


**Growth Pt on the surface of Pt nanorod and Thermal stability test (Fig. S4):** Pt nanorods (~ 2 mg) were dispersed in a mixture of Pt(acac)<sub>2</sub> (0.05mmol), ethylene glycol (1.86 mmol) and octadecylamine (15 mmol) in a two-neck round bottom flask (15 mL) with a magnetic stirring at 80 °C. After being evacuated for 10 min with stirring at 80 °C, the resulting solution was **kept at the same temperature for 20 h under Ar gas condition to form centepede-like Pt nanostructures.**

**[Thermal stability test]** The solution was recharged by CO gas and heated up to 200 °C. Finally, dark brown precipitates could be obtained by cooling down the solution to room temperature and then by centrifugation with added methanol / toluene (v / v = 15 / 15 mL).

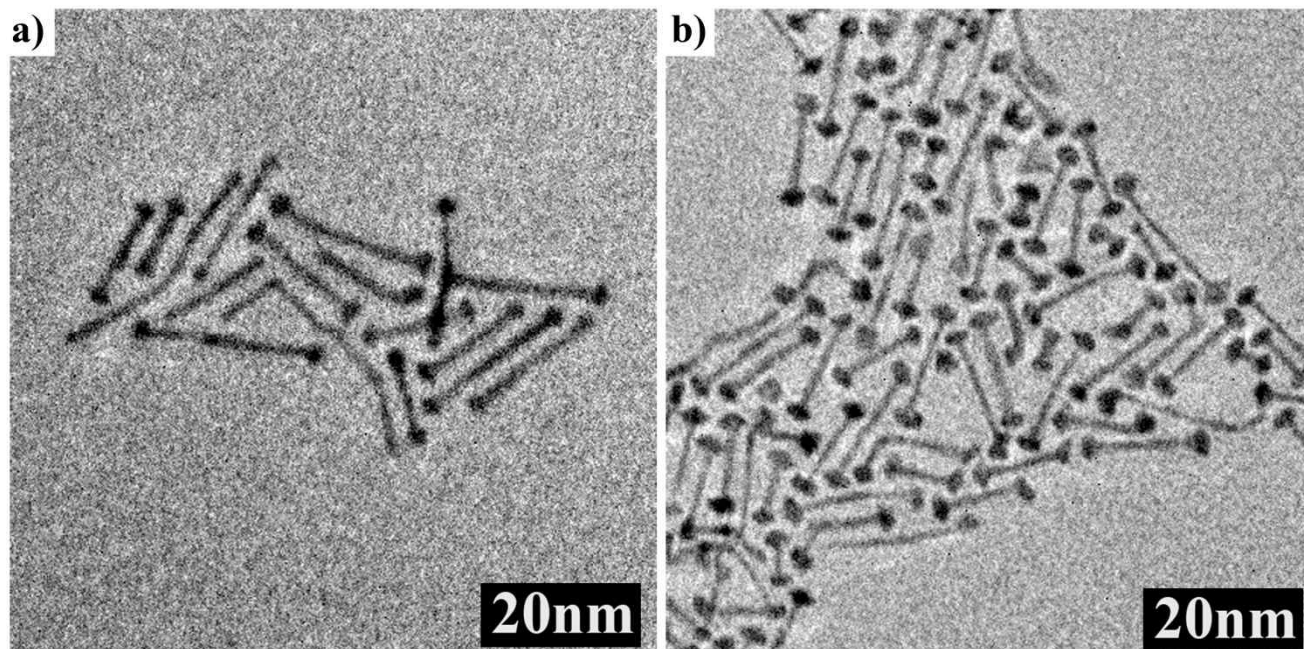


**Preparation of {Rh@Pt}-Pt-{Rh@Pt} nanodumbbells (Fig. 2):** Rh-Pt-Rh nanobarbells (2 mg) were dispersed in a mixture of Pt(acac)<sub>2</sub> (0.05mmol), ethylene glycol (1.86 mmol) and octadecylamine (15 mmol) in a two-neck round bottom flask (15 mL) with a magnetic stirring at 80 °C. After being evacuated for 10 min with stirring at 80 °C, the resulting solution was kept at the same temperature for 20 h under Ar gas condition. The solution was recharged by CO gas and heated up to 200 °C. Finally, dark brown precipitates could be obtained by cooling down the solution to room temperature and then by centrifugation with added methanol / toluene (v / v = 15 / 15 mL).

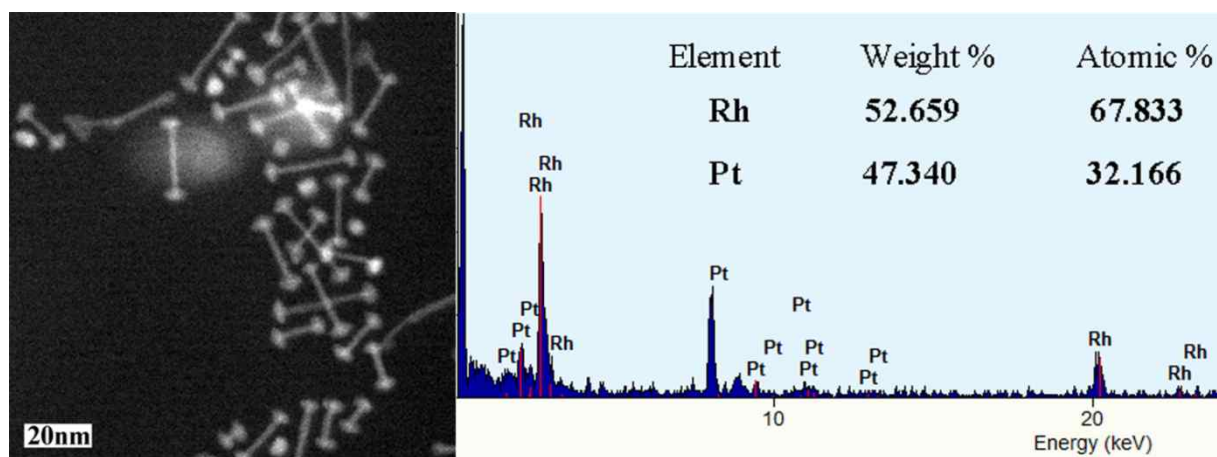


**Overgrowth of Pd on the Rh-Pt-Rh nanobarbells and Thermal stability test (Fig. S5):** The method is similar to the preparation of {Rh@Pt}-Pt-{Rh@Pt} nanodumbbells, except for the amount of Pd(acac)<sub>2</sub> (0.05 mmol) and initial vacuum treatment at 70 °C.

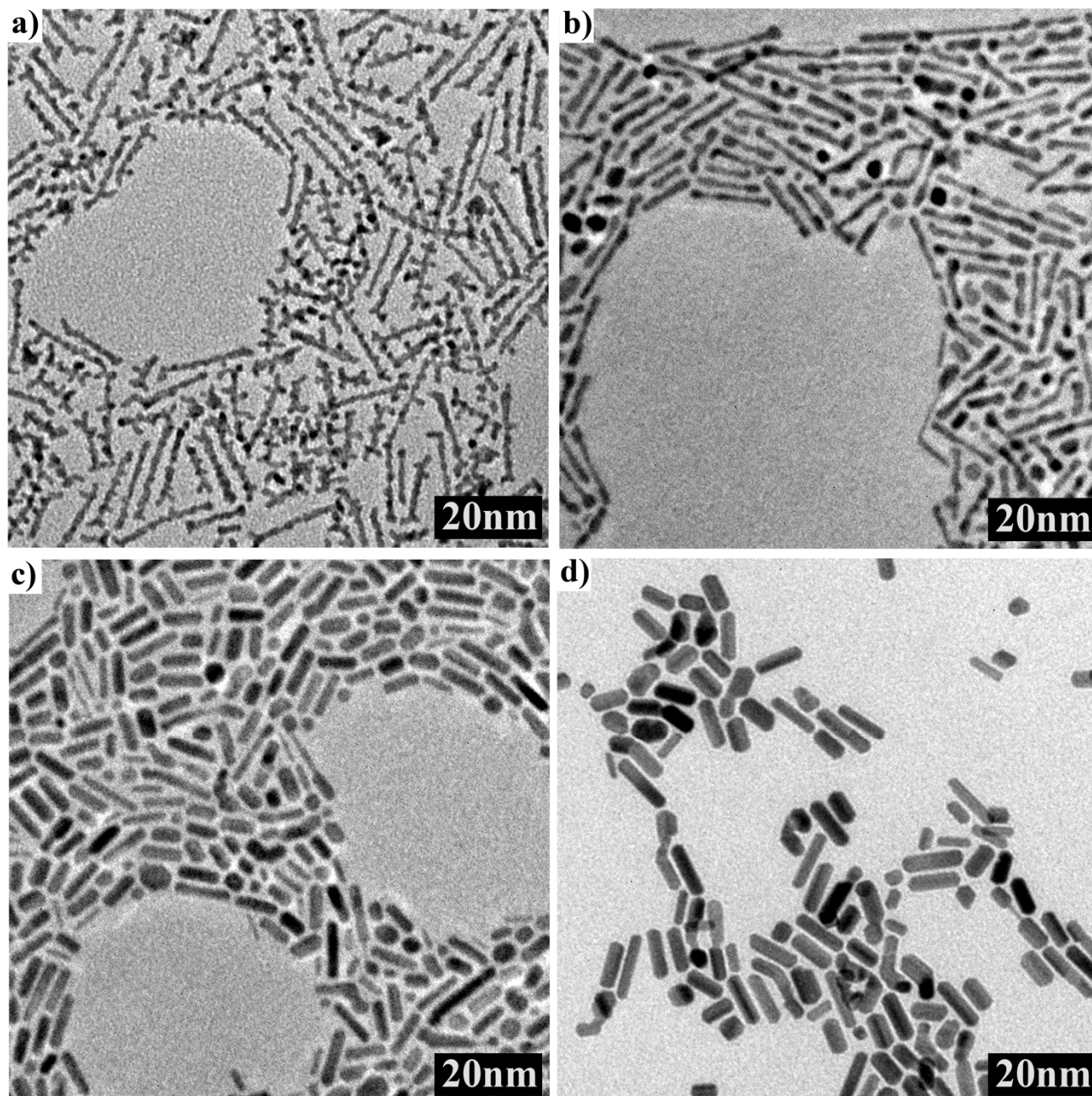
**Fig. S1.** TEM images of Rh-Pt-Rh nanobarbells a) before and b) after treatment at 200 °C under CO for 2 h.



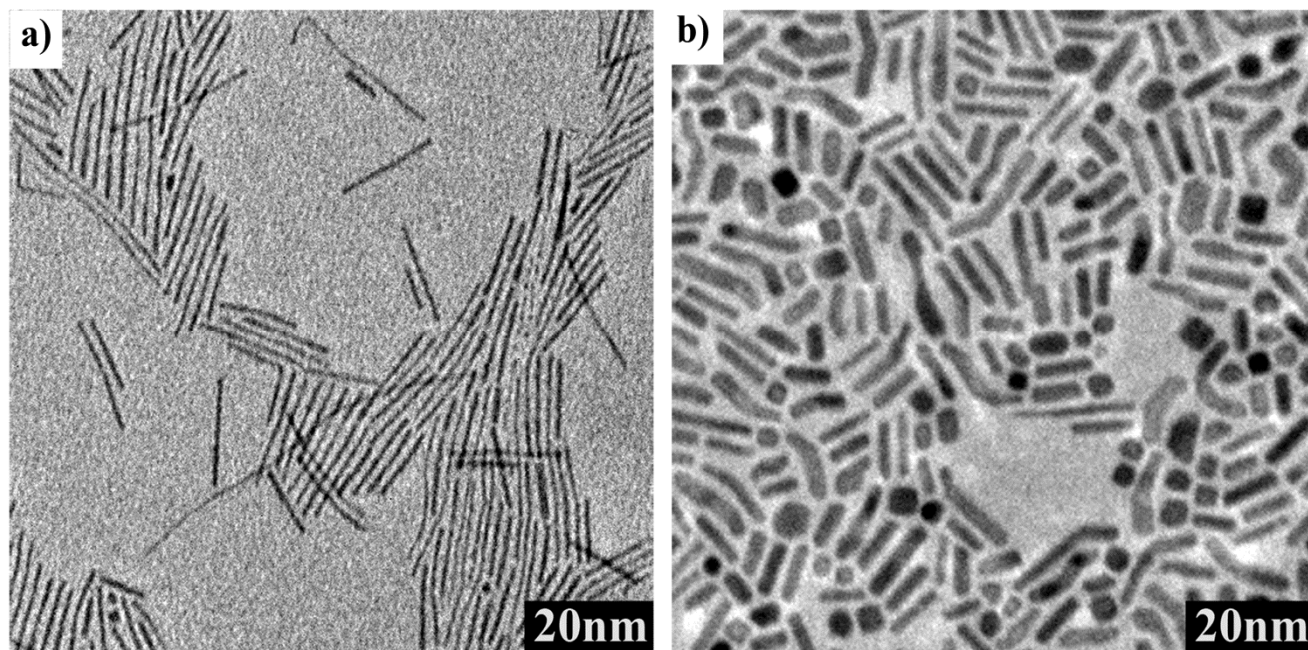
**Figure S2:** Energy dispersive X-ray spectrum of Rh-Pt-Rh barbells (NS 2) with TEM image



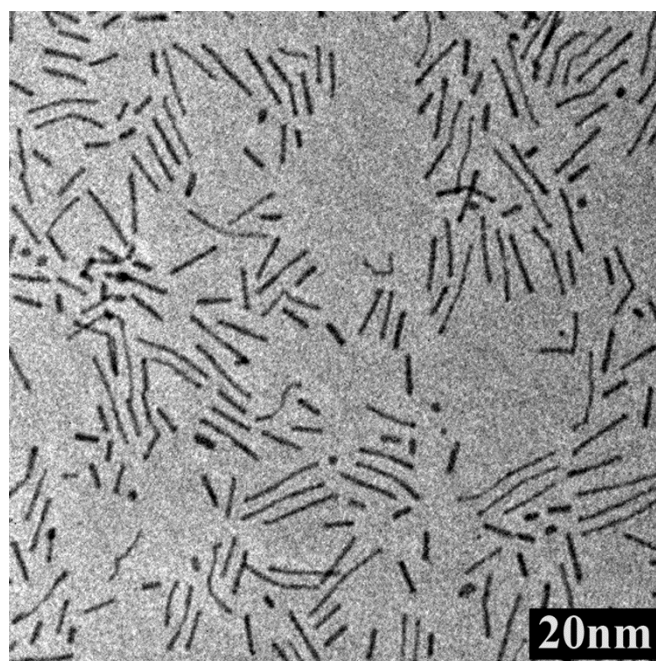
**Fig. S3.** a) TEM images of Pt nanorods with small Pt nanoparticles overgrown; b, c, d) The deformation of them at 200 °C under CO after 5 min, 10 min and 2 h. The worm-like Pt nanostructures are deformed to give short and thick nanorods under CO at elevated temperatures.



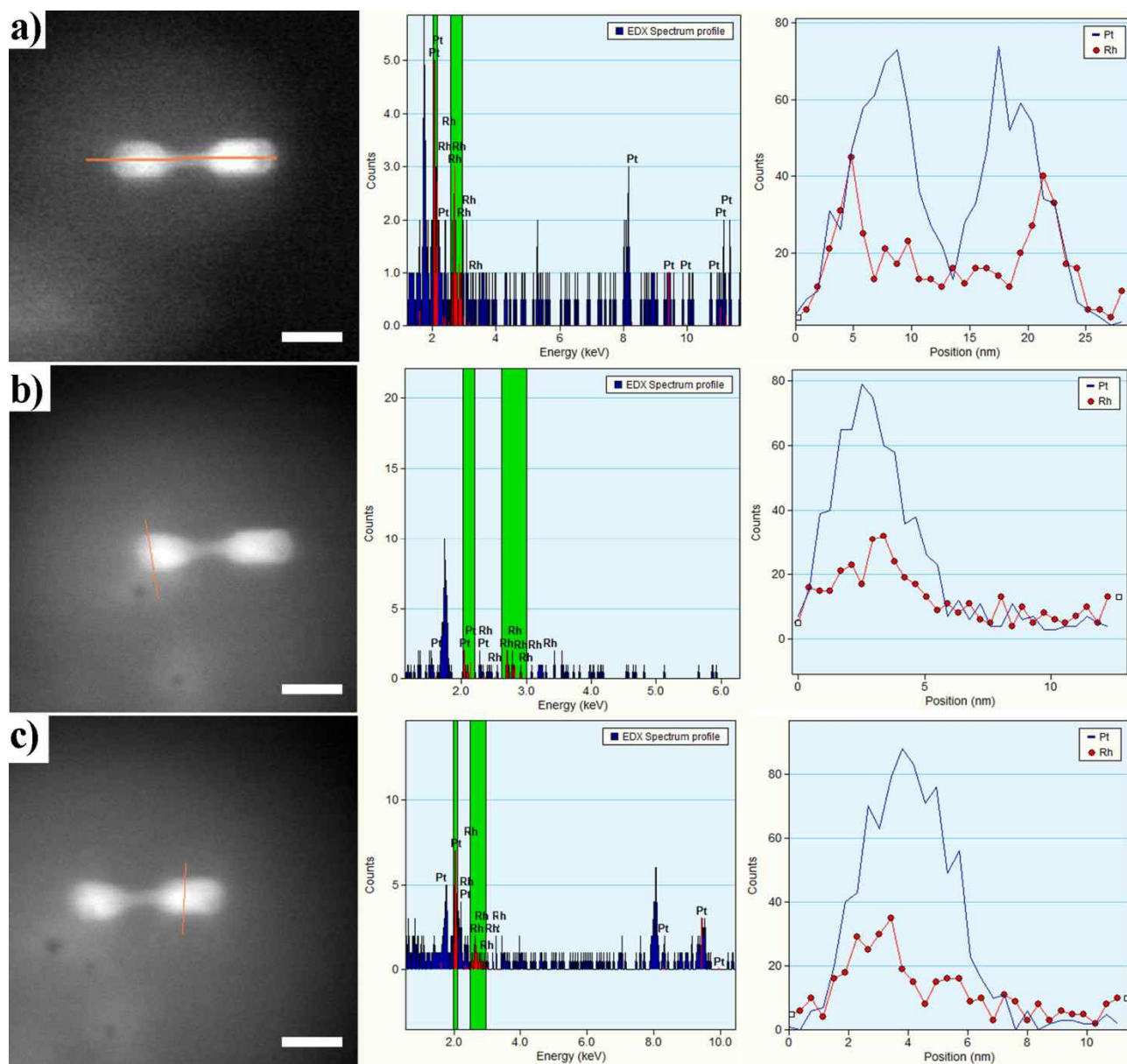
**Fig. S4. Deformation of Pt nanorods at elevated temperatures under CO.** a) TEM image of thin Pt nanorods; b) TEM image of Pt nanorods after being treated at 200 °C under CO for 1 h.



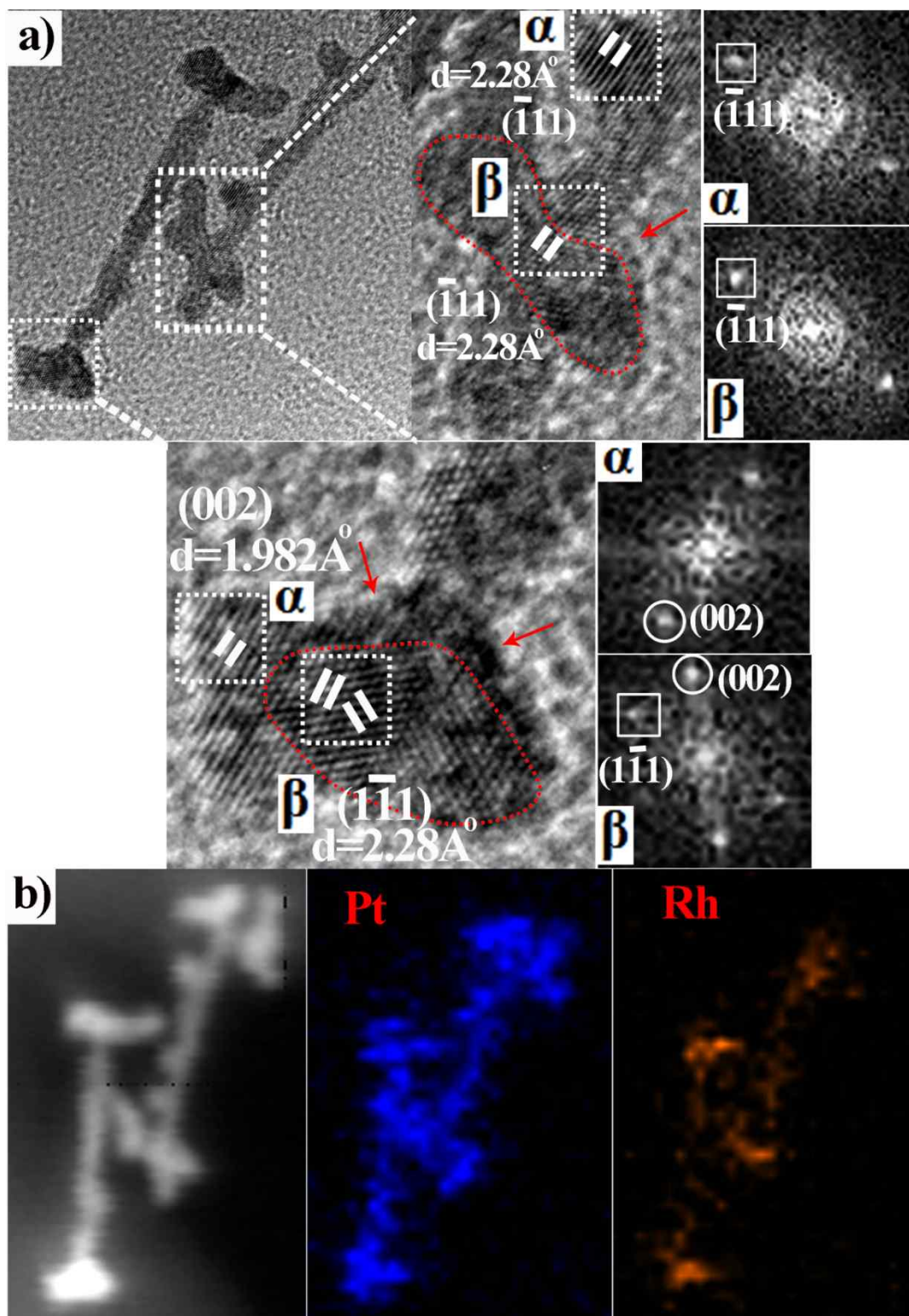
**Fig. S5.** TEM image of Pt nanorods after being treated at 200 °C under Ar for 2 h.



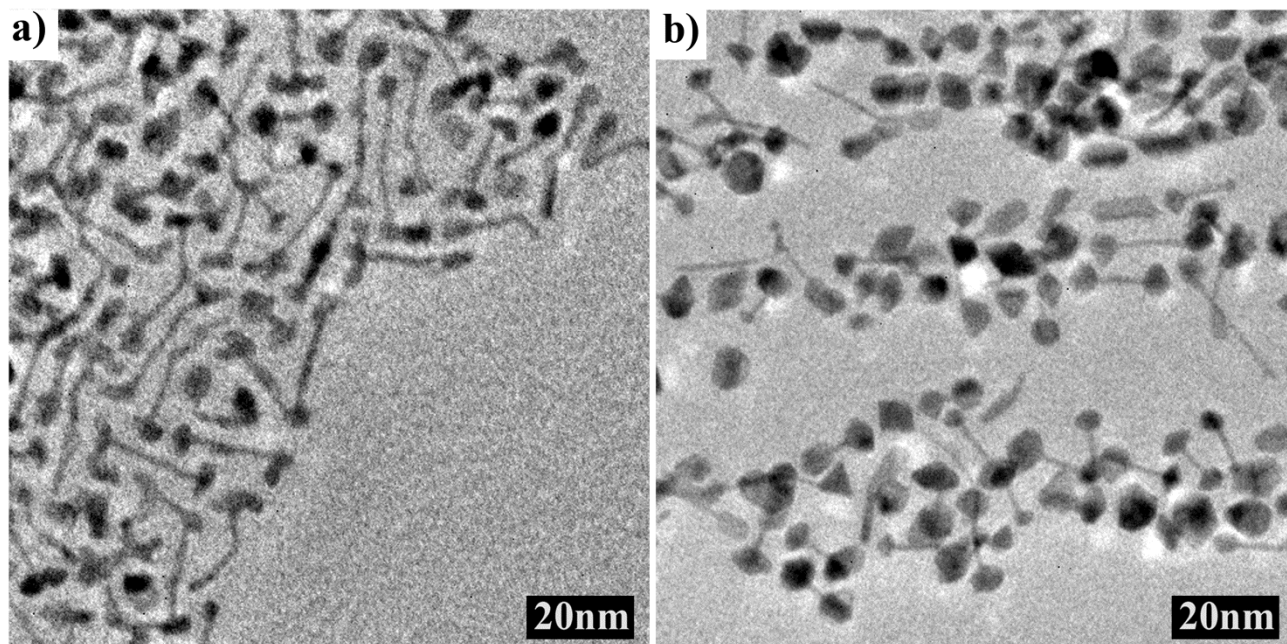
**Fig. S6.** HAADF STEM image of nanodumbbell of Pt bar and two Rh@Pt balls NPs with corresponding EDX data and element profile along with the red line: Scale bar equals 10 nm. The core-shell composition of Rh@Pt is clearly shown.



**Fig. S7. The presence of Pt bridge connecting the Rh tip and Pt nanorod.** a) HRTEM image of Rh-Pt-Rh nanobarbell with Pt overgrown (inset: magnified image of selected area;  $\alpha$  and  $\beta$ : FFTs of HRTEM images of selected area. Rh tip part is indicated by the red dotted line. Pt bridge connecting the Pt nanorod and Rh tip is shown by the red arrows.) and b) Elemental mapping of the nanoparticles in (a).



**Fig. S8.** a) TEM image of Pd-coated Rh-Pt-Rh nanobarbells; b) TEM image of the resulting nanostructures after 2 h treatment at 200 °C under CO for 2 h.



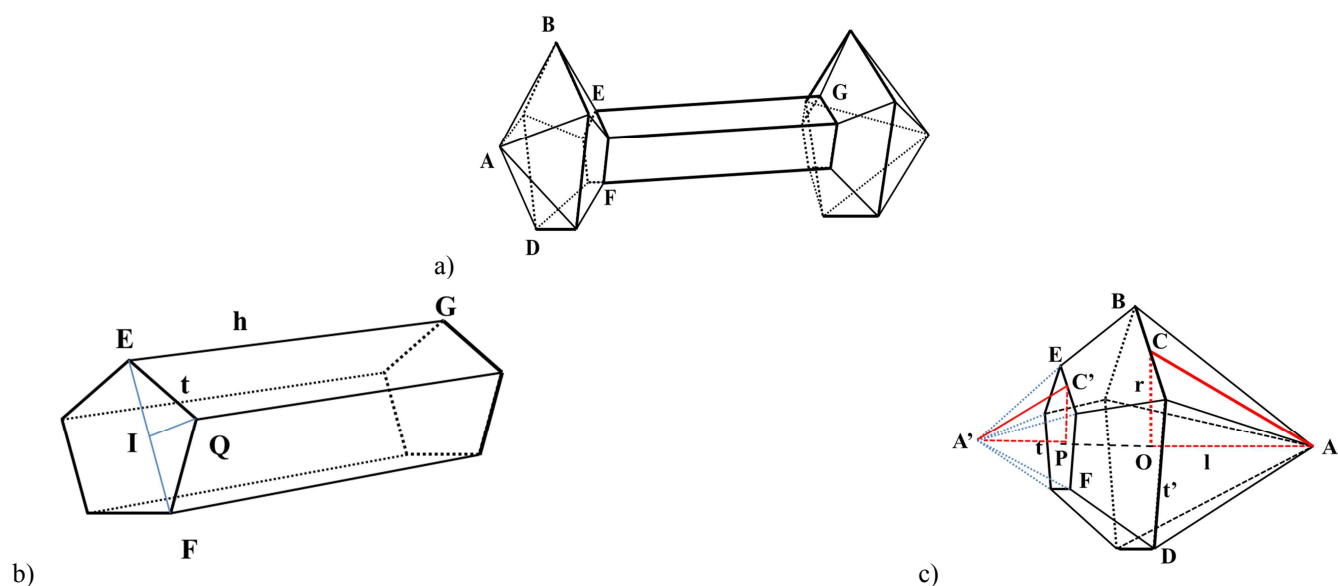


**Fig. S9.** Model of a) nanobarbell with Pt bar and Rh balls with b) a five-fold twinned Pt nanorod and c) two twinned Rh tips.

### Calculation of relative surface areas of Rh and Pt in Rh-Pt-Rh nanobarbell

Pt bar is right prism with pentagon base have side length  $t$  and  $h = EG$  is the height (figure S9a, b).

$$\rightarrow \text{Interior angle of pentagon base: } \frac{(n-2)\pi}{n} = \frac{(5-2)\pi}{5} = 0.6\pi$$

where  $n$ : number sided regular polygons.

$$\text{Angle } \widehat{EQI} = 0.3\pi$$

we can get  $EF$  from TEM image (see maximum length on the TEM image and see figure S9a).

$$\rightarrow t = \frac{EI}{\sin \widehat{EQI}} = \frac{EF}{2\sin(0.3\pi)}$$

→the surface area of Pt is lateral area of prism:

$$S_{\text{Pt}} = n \cdot t \cdot h = 5 \cdot \frac{EF}{2\sin(0.3\pi)} \cdot EG$$

$$\text{Volume: the volume of Pt bar: } V_{\text{Pt}} = \frac{n}{4} \frac{h \cdot t^2}{\tan \frac{\pi}{n}} = \frac{5 \cdot EG}{4 \tan \frac{\pi}{5}} \left( \frac{EF}{2\sin 0.3\pi} \right)^2$$

$$\text{Mass of Pt: } m_{\text{Pt}} = \rho_{\text{Pt}} V_{\text{Pt}}$$

$$\text{where } \rho_{\text{Pt}} = 21.45 \cdot 10^{-21} \text{ g} \cdot \text{nm}^{-3}: \text{density of Platinum}$$

Rh tip has 2 parts; one part is shaped as pyramid and the other one is frustum (see figure S8c).

$$\text{- Pyramid is pentagonal with base side length } t_1 = \frac{BD}{2\sin(0.3\pi)} \text{ and slant height AC}$$

$$AC = \sqrt{l^2 + r_1^2}$$

Where  $l$  is the pyramid altitude,  $l = AO$ ,  $r_l$  is the radius of the base.

$$r_1 = \frac{t_1}{2 \sin \frac{\pi}{n}} = \frac{BD}{4 \sin \frac{\pi}{5} \sin(0.3\pi)}$$

$$\rightarrow AC = \sqrt{AO^2 + \frac{BD^2}{(4 \sin(0.2\pi) \cdot \sin(0.3\pi))^2}}$$

→ lateral surface area of pyramid part:

$$S_{pyramid} = n \cdot \frac{1}{2} t_1 \cdot AC = 5 \cdot \frac{BD}{4 \sin(0.3\pi)} \sqrt{AO^2 + \frac{BD^2}{(4 \sin(0.2\pi) \cdot \sin(0.3\pi))^2}}$$

- Frustum part is the portion of a pyramid that lies between two parallel planes cutting it. Bases of frustum are pentagon with side  $t$  and  $t_1$  ( $t_1 > t$ ).

*Lateral surface area of frustum is lateral surface area of big pyramid (apex is A' and base is pentagon containing the point BDC, center O) subtraction lateral surface area of small pyramid (apex is A' and base is pentagon containing the point EFC', center P).*

$$\text{lateral surface area of big pyramid} = 5 \cdot \frac{BD}{4 \sin(0.3\pi)} \sqrt{A'O^2 + \frac{BD^2}{(4 \sin(0.2\pi) \cdot \sin(0.3\pi))^2}} = 5 \cdot \frac{BD}{4 \sin(0.3\pi)} \sqrt{AO^2 + \frac{BD^2}{(4 \sin(0.2\pi) \cdot \sin(0.3\pi))^2}}$$

Same method for calculation of pyramid part.

$$\rightarrow \text{lateral surface area of small pyramid} = n \cdot \frac{t \cdot A'C'}{2} = 5 \cdot \frac{EF}{4 \sin(0.3\pi)} \sqrt{A'P^2 + \frac{EF^2}{(4 \sin(0.2\pi) \cdot \sin(0.3\pi))^2}}$$

where  $A'P = A'O - OP = AO - OP$

$$\rightarrow \text{lateral surface area of small pyramid} = 5 \cdot \frac{EF}{4 \sin(0.3\pi)} \sqrt{(AO - OP)^2 + \frac{EF^2}{(4 \sin(0.2\pi) \cdot \sin(0.3\pi))^2}}$$

→ lateral surface area of frustum part:

$$S_{frustum \text{ parts}} = \frac{5}{4 \sin(0.3\pi)} \left( BD \sqrt{AO^2 + \frac{BD^2}{(4 \sin(0.2\pi) \cdot \sin(0.3\pi))^2}} - EF \sqrt{(AO - OP)^2 + \frac{EF^2}{(4 \sin(0.2\pi) \cdot \sin(0.3\pi))^2}} \right)$$

→ the surface area of Rh:

$$S_{Rh} = 2(S_{pyramid \text{ parts}} + S_{frustum \text{ parts}}) =$$

$$= \frac{5}{2 \sin(0.3\pi)} \left( 2 \cdot BD \sqrt{AO^2 + \frac{BD^2}{(4 \sin(0.2\pi) \cdot \sin(0.3\pi))^2}} - EF \sqrt{(AO - OP)^2 + \frac{EF^2}{(4 \sin(0.2\pi) \cdot \sin(0.3\pi))^2}} \right)$$

Volume:

$$\text{Volume of pyramid part: } V_{pyramid} = \frac{n}{12} l \cdot t_1^2 \omega t \frac{\pi}{n} = \frac{5}{12} AO \left( \frac{BD}{2 \sin(0.3\pi)} \right)^2 \omega t \frac{\pi}{5} = \frac{5\omega t \frac{\pi}{5}}{48(\sin(0.3\pi))^2} AO * BD^2$$

Volume of frustum is volume of big pyramid (apex is A' and base is pentagon containing the point BDC, center O) subtraction volume of small pyramid (apex is A' and base is pentagon containing the point EFC', center P).

$$\rightarrow V_{frustum} = \frac{5}{12} A'O \left( \frac{BD}{2 \sin(0.3\pi)} \right)^2 \omega t \frac{\pi}{5} - \frac{5}{12} A'P \left( \frac{EF}{2 \sin(0.3\pi)} \right)^2 \omega t \frac{\pi}{5} = \frac{5\omega t \frac{\pi}{5}}{48(\sin(0.3\pi))^2} [AO * BD^2 - (AO - OP)EF^2]$$

$$V_{Rh} = 2(V_{pyramid} + V_{frustum}) = 2 \left\{ \frac{5\omega t \frac{\pi}{5}}{48(\sin(0.3\pi))^2} AO * BD^2 + \frac{5\omega t \frac{\pi}{5}}{48(\sin(0.3\pi))^2} [AO * BD^2 - (AO - OP)EF^2] \right\}$$

$$= \frac{5\omega t \frac{\pi}{5}}{24(\sin(0.3\pi))^2} [2AO * BD^2 - (AO - OP)EF^2]$$

Mass of Rh:  $m_{Rh} = \rho_{Rh} \cdot V_{Rh}$  with  $\rho_{Rh} = 12.41 * 10^{-21} \text{ g.nm}^{-3}$ : density of Rhodium .

Apply for Rh-Pt-Rh nanobarbell (NS 2): (standard deviations measured from 50 NPs)

$$\overline{AO} = 2.77 \pm 0.21 \text{ nm}; \overline{OP} = 0.92 \pm 0.09 \text{ nm}; \overline{BD} = 6.04 \pm 0.44 \text{ nm};$$

$$\overline{EF} = 2.02 \pm 0.18 \text{ nm}; \overline{EG} = 15.9 \pm 1.6 \text{ nm}$$

$$\rightarrow S_{Pt} = 5 \cdot \frac{\overline{EF}}{2 \sin(0.3\pi)} \cdot \overline{EG} = 5 \frac{2.02}{\sin(0.3\pi)} 15.9 \doteq 99.30(\text{nm}^2)$$

$$S_{Rh} = \frac{5}{2 \sin(0.3\pi)} \left( 2 \cdot \overline{BD} \sqrt{AO^2 + \frac{BD^2}{(4 \sin(0.2\pi) \cdot \sin(0.3\pi))^2}} - \overline{EF} \sqrt{(AO - OP)^2 + \frac{EF^2}{(4 \sin(0.2\pi) \cdot \sin(0.3\pi))^2}} \right)$$

$$= \frac{5}{2 \sin(0.3\pi)} \left( 2 * 6.04 \sqrt{2.77^2 + \frac{6.04^2}{(4 \sin(0.2\pi) \cdot \sin(0.3\pi))^2}} - 2.02 \sqrt{(2.77 - 0.92)^2 + \frac{2.02^2}{(4 \sin(0.2\pi) \cdot \sin(0.3\pi))^2}} \right) \doteq 144.17(\text{nm}^2)$$

$$\frac{S_{Rh}}{S_{Pt}} = \frac{147.19}{99.30} \doteq 1.45$$

$$V_{Pt} = \frac{5 \cdot \overline{EG}}{4 \tan \frac{\pi}{5}} \left( \frac{\overline{EF}}{2 \sin 0.3\pi} \right)^2 = \frac{5 * 15.9}{4 \tan \frac{\pi}{5}} \left( \frac{2.02}{2 \sin 0.3\pi} \right)^2 \doteq 42.68(\text{nm}^3)$$

$$\rightarrow m_{Pt} = \rho_{Pt} * V_{Pt} = 21.45 * 10^{-21} * 42.68 \doteq 0.915 * 10^{-18}(\text{g})$$

$$V_{Rh} = \frac{5\omega t \frac{\pi}{5}}{24(\sin(0.3\pi))^2} [2AO * BD^2 - (AO - OP)EF^2] = \frac{5\omega t \frac{\pi}{5}}{24(\sin(0.3\pi))^2} [2 * 2.77 * 6.04^2 - (2.77 - 0.92)2.02^2]$$

$$\cong 85.38(\text{nm}^3)$$

$$\rightarrow m_{\text{Rh}} = \rho_{\text{Rh}} * V_{\text{Rh}} = 12.41 * 10^{-21} * 85.38 \cong 1.060 * 10^{-18}(\text{g})$$

$$\text{weight \% of Pt} = \left( \frac{m_{\text{Pt}}}{m_{\text{Pt}} + m_{\text{Rh}}} * 100 \right) \% = \left[ \frac{0.915 * 10^{-18}}{(0.915 + 1.060) * 10^{-18}} * 100 \right] \% \cong 46.33\%$$

$$\text{weight \% of Rh} = \left( \frac{m_{\text{Rh}}}{m_{\text{Pt}} + m_{\text{Rh}}} * 100 \right) \% = \left[ \frac{1.060 * 10^{-18}}{(0.915 + 1.060) * 10^{-18}} * 100 \right] \% \cong 53.67\%$$

These values of 46 wt % and 54 wt % are only slightly different from the values (47 wt% and 53 wt%) obtained by EDAX measurements (See Fig. S2). However, for the qualitative understanding of the electrochemical study, these approximate surface area values were sufficient.

***Apply for Thermally treated NS 2 (NS 3):***

$$\overline{\text{AO}} = 2.90 \pm 0.28 \text{ nm}; \overline{\text{OP}} = 0.96 \pm 0.10 \text{ nm}; \overline{\text{BD}} = 6.50 \pm 0.43 \text{ nm}; \overline{\text{EF}} = 2.18 \pm 0.17 \text{ nm}; \overline{\text{EG}} = 13.6 \pm 1.53 \text{ nm}$$

$$S_{\text{Pt}} \cong 91.68(\text{nm}^2)$$

$$S_{\text{Rh}} \cong 164.52(\text{nm}^2)$$

$$\frac{S_{\text{Rh}}}{S_{\text{Pt}}} = \frac{164.52}{91.68} \cong 1.79$$

## Electrochemical experiment and instruments

Glassy carbon disk electrode (GCE) (dia. 3 mm, CH Instruments, Austin, TX) were used as support for nanostructures. GCE was prepared by polishing with 1.0 and 0.3  $\mu\text{m}$  alumina powder on a polishing cloth (Buehler) followed by sonication in water for 5 min. The electrodes were then rinsed with water and dried. 20  $\mu\text{L}$  of Nafion solution (1/100 diluted from 5 wt. % stock solution, Aldrich) was dropped on the cleaned GCE and dried for 30 min. The 5 mg of prepared nanostructures were dispersed in 7 mL of methanol by 10 min of sonication. Then 20  $\mu\text{L}$  of the nanostructure solution was dropped on the nafion coated GCE and dried for at least 1 h. The electrochemical experiment was performed using a CHI model 660d potentiostat (CH Instruments, Austin, TX). The three-electrode electrochemical cell consisted of a modified GC working electrode, an Au wire counter electrode, and a Hg/Hg<sub>2</sub>SO<sub>4</sub>, K<sub>2</sub>SO<sub>4</sub>(sat'd) reference electrode (0.64 V vs. NHE) was used. All the potential in this paper were reported vs. NHE.

## Electrocatalytic activity for oxygen reduction reaction (ORR) and electrochemically active surface area (ECSA)

Glassy carbon electrodes (GCEs) modified with nanostructures (NS 1: five-fold twined Pt nanorod, NS 2: nanodumbbell of Pt bar and two Rh balls NPs, NS 3: Thermally treated NS 2, NS 4: nanodumbbell of Pt bar and two Rh@Pt balls NPs) were prepared as described in the experimental section, and their electrocatalytic properties for the oxygen reduction reaction (ORR) were evaluated using cyclic voltammetry (CV). Cyclic voltammograms (CVs) were acquired in an O<sub>2</sub>- or Ar-saturated aqueous electrolyte solution containing 0.5 M H<sub>2</sub>SO<sub>4</sub>. Before the CVs were obtained, the electrodes were activated by scanning the potential between 1.6 V and 0.0 V (vs. NHE) several times in the same electrolyte solution. Fig. 1 shows the nanostructure modified GCE exhibits a well-defined peak around 0.7 V that corresponds to the ORR. The onset potentials of ORR were around 0.84 V at both NS 1 and NS 4. Slightly negative shifted onset potentials, 0.75 V were obtained at both NS 2 and NS 3. Pt NPs modified GCE. The difference in onset potential is caused by the difference composition. The surface of nanostructure NS 1 and NS 4 are consisted of only Pt atoms but NS 2 and NS 3 are consisted of Pt and Rh atoms.

For electrocatalytic reactions, it is important to know the electrochemically active surface area (ECSA) of the catalyst. We determined this value experimentally using the hydrogen adsorption/desorption method <sup>[2]</sup>. The broad peaks between 0.30 V and -0.05 V shown in Fig. 1 are characteristic of hydrogen adsorption and desorption. We calculated the active surface area of the Pt and Rh catalyst on the basis of the charge associated with the hydrogen adsorption region (cathodic current between 0.35 V and 0.0 V) in Ar- Saturated electrochemical cell (data is not shown here). After subtraction of the background charge, the

total charge was obtained; 23.4  $\mu\text{C}$  for nanostructure NS 1, 73.1  $\mu\text{C}$  for nanostructure NS 2, 25.6  $\mu\text{C}$  for nanostructure NS 3, and 60.3  $\mu\text{C}$  for nanostructure NS 4, which corresponds respectively to 0.111, 0.337, 0.118, and 0.287  $\text{cm}^2$  of ECSA assuming that hydrogen desorption yields 210  $\mu\text{C}/\text{cm}^2$  of Pt surface area and hydrogen desorption yields 221  $\mu\text{C}/\text{cm}^2$  of Rh surface area [2,3].

**Fig. S10.** Cyclic voltammograms of nanostructures (NS 1: five-fold twined Pt nanorod, NS 2: nanodumbbell of Pt bar and two Rh balls NPs, NS 3: Thermally treated NS 2, NS 4: nanodumbbell of Pt bar and two Rh@Pt balls NPs) modified GCE in (a)  $\text{O}_2$ -, (b) Ar- saturated 0.5 M  $\text{H}_2\text{SO}_4$  electrolyte solution. Scan rate was 50 mV/s.

The data was obtained in  $\text{O}_2$ -saturated condition. Therefore the ORR also happened at the same potential region. Because of the off-set current (reduction current) by the ORR, the hydrogen desorption peak positioned near the zero or negative current region. In Ar-saturated condition, the hydrogen desorption peak of all the samples are positive values. Rh showed bad CO-tolerance [reference 36, *Int. J. Electrochem. Sci.*, 3(2008) 970-979]. That's the reason why the backward peak disappeared in NS-2 or NS-3 as compared with NS-1 or NS-4 which do not show Rh on the surface. The NS-3 is prepared from NS-2 with thermal treatment under the CO. The CO treatment might have poisoned the Rh on the NS-3, therefore responsible for the lower current.

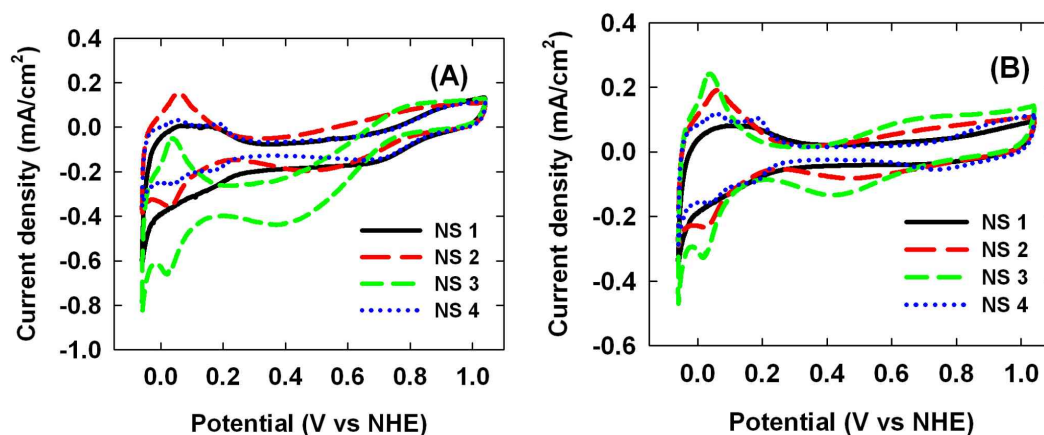


**Fig. S11.** Chronoamperometry curves at 0.84 V (vs NHE) of nanostructures (NS 1: five-fold twined Pt nanorod, NS 2: nanodumbbell of Pt bar and two Rh balls NPs, NS 3: Thermally treated NS 2, NS 4: nanodumbbell of Pt bar and two Rh@Pt balls NPs) modified GCE in 0.5 M MeOH + 0.5 M H<sub>2</sub>SO<sub>4</sub> electrolyte solution.

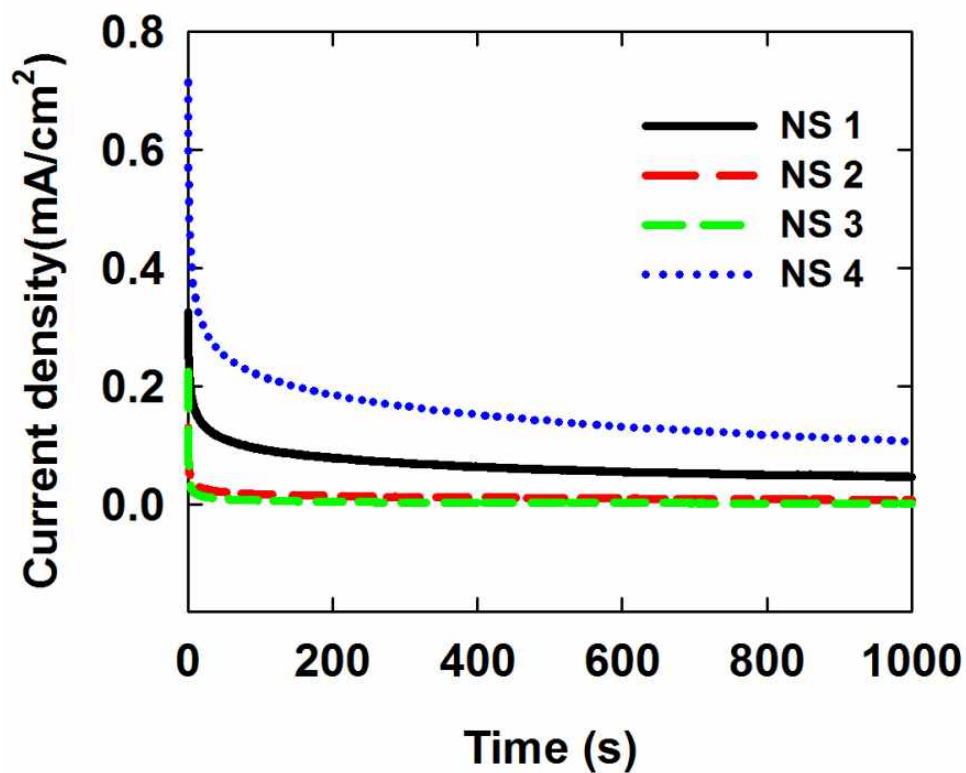
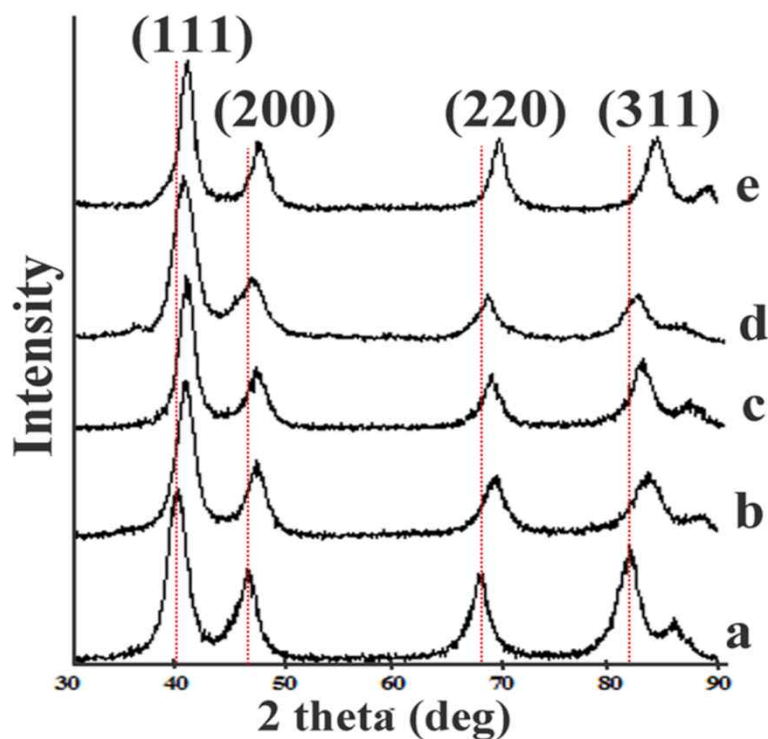


**Fig. S12.** X-ray diffraction patterns: a) thin Pt nanorod (JCPDS card no. 04-0802); b) Rh-Pt -Rh nanobarbell; c) Pt-coated Rh-Pt -Rh nanobarbell; d) {Rh@Pt}-Pt-{Rh@Pt} nanodumbbell; e) Rh nanoparticles (JCPDS card no. 01-1214).



#### Reference

1. J. Yoon, N. T. Khi, H. Kim, B. Kim, H. Baik, S. Back, S. Lee, S. W. Lee, S. J. Kwon, K. Lee, *Chem. Commun.* 2013, **49**, 537.
2. T. Biegler, D. A. J. Rand, R. Woods, *J. Electroanal. Chem.* 1971, **29**, 269.
3. R. Woods, in *Electroanalytical Chemistry: A Series of Advances, Vol. 9* (Ed.: A. J. Bard), Marcel Dekker, New York, 1974, pp 1-162.